



RESEARCH ARTICLE

A high-precision and efficient algorithm for space-based ADS-B signal separation

Yan Bi,^{1,2} Renbiao Wu,² and Qiongqiong Jia²

¹School of Electrical and Information Engineering, Tianjin University, Tianjin, China

²Tianjin Key Lab for Advanced Signal Processing, Civil Aviation University of China, Tianjin, China.

Corresponding author: Renbiao Wu; Email: rbwu@cauc.edu.cn

Received: 27 June 2021; **Accepted:** 3 May 2023; **First published online:** 16 June 2023

Keywords: ADS-B; space-based ADS-B system; array antenna; signal separation

Abstract

Space-based automatic dependent surveillance-broadcast (ADS-B) receivers can cover thousands of aircraft, each transmitting 6·2 signals per second. As a result, ADS-B signals are very prone to overlap. When the number of aircraft covered by a receiver reaches 3,000, about 90 % of the signals will be overlapping. Overlapped signals can reduce the decoding accuracy of receivers, so that aircraft information cannot be accurately transmitted to the air traffic control (ATC) surveillance system, hence threatening aviation flight safety. It is necessary to propose signal separation algorithms for space-based ADS-B systems. An orthogonal projection linear constrained minimum variance (OPLCMV) algorithm is proposed, which can separate two signals simultaneously based on the linearly constrained minimum variance algorithm by exploiting the characteristics of overlapped signals. Compared with the state-of-the-art extended projection algorithm and the fast independent component analysis algorithm, the OPLCMV method has a higher decoding accuracy for multiple overlapping signals with a small direction difference of arrival or frequency shift. Moreover, the OPLCMV algorithm has a low computational complexity when the number of overlapped signal sources is less than seven.

1. Introduction

Automatic dependent surveillance-broadcast (ADS-B) has been identified by the International Civil Aviation Organization (ICAO) as the next-generation air traffic control (ATC) surveillance system (Ali et al., 2017). This system allows aircraft to obtain aircraft number, position, altitude, speed, and other information using airborne equipment and the global navigation satellite system (GNSS). The information is then encoded into messages based on the data communication link format and broadcast automatically. The ADS-B system uses air–ground and air–air data communication to complete information transmission and traffic monitoring (Ali, 2016; Baek et al., 2016; Mangali and Bagmare, 2017; Zhou et al., 2017). ADS-B Out is enforced to maintain surveillance of aviation operations in Australia, China, Europe and the United States. To overcome the limitations of traditional radar and ground-based ADS-B systems in monitoring airspaces like oceans, polar regions and deserts, ADS-B receivers are placed on low-orbiting satellites in space-based ADS-B systems (Blomenhofer et al., 2012; Knudsen et al., 2014; Baker, 2019). The space-based ADS-B system can cover 100 % of the global airspace and effectively monitor the flight status of each aircraft in the airspace. When an aircraft is on a dangerous or unusual course, it can be located and rescued in the shortest time to avoid accidents like those that befell flights MH370 and AF447. Therefore, the space-based ADS-B system has great significance to the development of aviation. Currently, the world's first space-based ADS-B system (Garcia et al., 2017) has been completed by the Aireon Company in the United States. It has provided aircraft surveillance

services for multiple countries and regions since 2020. Other space-based ADS-B systems are also actively deployed in China (Wu et al., 2016; Chen et al., 2020), Canada (Vincent and Freitag, 2019), Denmark (Nies et al., 2018), Germany (Werner et al., 2014), and other countries.

The existing space-based ADS-B system has a satellite orbit altitude range of 400 to 1,000 km (Carandente and Rinaldi, 2014; Werner et al., 2014; Wu et al., 2016; Vincent and Freitag, 2019; Chen et al., 2020), and the airspace radius covered by a single receiver has increased from 200 km to 1,900 km (Werner et al., 2014; Garcia et al., 2017, 2018), so the number of aircraft covered by a space-based ADS-B receiver has increased significantly and continues to grow with the expansion of the aviation industry. When a receiver covers too many aircraft, the ADS-B signals transmitted from different aircraft are likely to reach the receiver at the same time, causing their time domain waveforms to overlap with each other. These signals are known as overlapped signals. Overlapped signals can reduce the decoding accuracy of common receivers and cause the loss or incorrect decoding of ADS-B signals, which makes the ATC system unable to monitor aircraft operation accurately and affects aviation flight safety. Therefore, it is critical to separate ADS-B overlapped signals. Compared with the ground-based system, the ADS-B signal overlap problem is more serious in space-based ADS-B systems. This is mainly reflected in two aspects. Firstly, the space-based ADS-B system has more multiple overlapping signals than the ground-based ADS-B system. Since the number of aircraft covered by a space-based receiver is larger than that of a ground-based receiver (Blomenhofer et al., 2012), the probability of multiple signals overlapping will be increased. For example, to ensure that the correct reception probability of the ADS-B signal is no less than 90 %, the ground-based receiver only needs to separate two overlapping signals, while the space-based receiver should be able to separate six or more overlapping signals (Liu et al., 2016). Secondly, the direction difference of arrival (DDOA) between space-based ADS-B overlapped signals is smaller than that of ground-based ADS-B overlapped signals, since the distance between the aircraft and the satellite receiver is much farther than that between the aircraft and the ground receiver (Zhang et al., 2019). To summarise, the space-based ADS-B system faces a more severe signal overlap issue, and there is an urgent need to develop signal separation algorithms tailored for the space-based ADS-B overlapped signals.

So far, several separation algorithms have been proposed for space-based ADS-B overlapped signals, and they can be divided into three main categories. One approach is to design a multi-beam antenna that can divide the airspace covered by the receiver into several regions with each beam covering a designated area to reduce the probability of multiple overlapping signals. However, there may be a few overlapping signals under a single beam, and the DDOA is too small to separate these signals (Bettray et al., 2013; Yu et al., 2019). The second approach is based on a single antenna (Galati et al., 2015; Yu et al., 2018; Zhang, 2018). They utilise time-frequency analysis methods to separate the overlapped signals based on the frequency shifts between them. Nowadays, this approach can only effectively separate two or three overlapping signals. The third approach uses an array antenna to separate signals, such as fast independent component analysis (FastICA) (Zhang et al., 2019), Manchester decoding algorithm (MDA) (Petrochilos and Van Der Veen, 2007), extended projection algorithm (EPA) (Petrochilos et al., 2009), and alternating direction method of multipliers (ADMM) (Wang et al., 2019). The spatial and temporal characteristics of ADS-B signals are exploited by these methods, so multiple overlapping signals can be separated effectively. Among all the ADS-B signal separation methods, this approach can separate the most overlapping signals. The FastICA algorithm separates overlapped signals by exploiting the non-Gaussian nature of the ADS-B signal. It is insensitive to the time differences of arrival (TDOAs) and DDOAs between the overlapping signals. However, the mixing matrix of the overlapped signal as the initial value of the weighting matrix needs to be known, since the initial value determines the accuracy and convergence of the algorithm, which is difficult to achieve in practice. Therefore, the existing FastICA method is only applicable to two overlapping signals and has poor performance on multiple overlapping signals. The MDA is suitable for overlapped signals with a high input signal-to-noise ratio (SNR) and small TDOAs, which is insensitive to the DDOAs. The performance of the algorithm deteriorates when the input SNRs of overlapping signals are less than 10dB or the TDOAs are greater than 30 μ s. Moreover, this method is also not suitable for multiple overlapping signals. Different from the above methods,

the EPA can separate two to eight overlapping signals through real data verification, but the separation accuracy is only 63 % when the number of overlapped signal sources exceeds four. Furthermore, the EPA needs to estimate the samples only containing one signal in the overlapped signals. When the TDOAs between overlapping signals are less than 4 μ s, the decoding accuracy of the algorithm decreases. The ADMM algorithm can separate overlapped signals using only one non-overlapping snapshot. However, the ADMM algorithm is inferior to the EPA when the TDOAs between overlapping signals are greater than 4 μ s. In conclusion, the existing space-based ADS-B separation algorithms have a lower decoding accuracy for multiple overlapping signals or the small DDOAs between overlapped signals.

To solve the space-based ADS-B signal overlap problem, an orthogonal projection linear constrained minimum variance (OPLCMV) algorithm based on array antennas is proposed in this paper. Firstly, the single-signal parts of the overlapped signal are identified based on the time-domain characteristics of the ADS-B overlapped signal. Secondly, the steering vectors of the first and last signals in the overlapped signal are estimated using these single-signal parts, and the separation matrix is calculated using the linearly constrained minimum variance (LCMV) algorithm. Then, both the first and last signals in the overlapped signal are separated simultaneously. Thirdly, the remaining overlapping signals are extracted by projecting the overlapped signal onto the orthogonal space of the separated signals. Finally, the above steps are repeated until all signals have been successfully separated. The method is evaluated in terms of the number of overlapped signal sources, the DDOAs and frequency shifts between the overlapped signal, the element number of the receiving array antenna, and the amount of computation. The OPLCMV algorithm can separate multiple overlapping signals and has a higher decoding accuracy for small DDOAs and frequency shifts between overlapped signals.

The rest of the paper is organised as follows. Section 2 proposes the main problem of the space-based ADS-B signal separation. Section 3 describes the proposed method. Experimental results and discussions are presented in Section 4. Section 5 summarises the advantages and disadvantages of the OPLCMV algorithm and its applicable conditions.

2. The problem of space-based ADS-B signal separation

2.1. High probability of multiple overlapping signals

The space-based ADS-B receiver covers a large number of aircraft in the airspace and receives an average of 6 · 2 signals per second from each aircraft. When the number of aircraft covered by the receiver reaches 3,000, according to the message collision probability of space-based ADS-B receiver established in the literature (Liu et al., 2018), 90 % of the received signals are overlapped signals. Meanwhile, according to the overlapped signal probability model established in the literature (Liu et al., 2016), a maximum of 13 signals can overlap in an overlapped signal. Multiple overlapping signals are therefore prone to appear in space-based ADS-B systems. To ensure the correct reception probability with no less than 90 %, the space-based ADS-B receiver should be able to separate at least six overlapping signals. However, most of the existing ADS-B signal separation methods (Yu et al., 2018; Zhang et al., 2019) can only effectively separate two or three overlapping signals, only the EPA (Petrochilos et al., 2009) can separate multiple overlapping signals, but it can only separate four overlapping signals with high precision.

2.2. Small DDOAs between overlapped signal

Currently, the first and only space-based ADS-B system in the world has been established by Aireon Company and the satellite orbit altitude of this system is 780 km. Assuming two civil aviation aircraft flying on adjacent routes with a maximum cruising altitude of 12 km, their minimum lateral separation can be up to 40 n miles (when flying over the ocean) (Lu et al., 2021). If the ADS-B signals emitted by the two aircraft overlap, the largest DDOA between the overlapped signal is approximately 5 · 52°. However, if the two aircraft are flying at different vertical altitudes, the DDOA can be 0°. The larger the number of overlapped signal sources, the higher the probability of small DDOA between overlapped

signal. Many algorithms are robust to the DDOA for ADS-B signal separation, such as projection algorithm single antenna (Galati et al., 2015) and MDA (Petrochilos and Van Der Veen, 2007). But these algorithms can only separate two or three overlapping signals.

In summary, the main problem of space-based ADS-B signal separation is that the existing ADS-B signal separation algorithms cannot solve the above two problems simultaneously. They can only separate multiple overlapping signals with a large DDOA, or separate fewer overlapping signals with a small DDOA. The proposed OPLCMV algorithm can separate multiple overlapping signals and also has higher decoding accuracy than existing algorithms when the DDOA is small. It is suitable for the space-based ADS-B signal separation problem.

3. OPLCMV algorithm

3.1. Space-based ADS-B overlapped signal model

Assume an ADS-B overlapped signal is received, and the signal is overlapped by d independent ADS-B signal sources. The receiver uses an m -element antenna array with arbitrary array manifold. The time domain expression of the overlapped signal can be expressed as

$$\mathbf{X} = \mathbf{A}\mathbf{S} + \mathbf{N} \quad (1)$$

where $\mathbf{X} = [\mathbf{x}_1 \mathbf{x}_2 \dots \mathbf{x}_L]$ is the $m \times L$ dimensional received signal matrix, and $\mathbf{x}_i = [x_{1,i} \ x_{2,i} \ \dots \ x_{m,i}]^T$ is the i -th snapshot of the received signal matrix, $i = 1, 2, \dots, L$. L is the number of received snapshots. \mathbf{A} is the steering vector matrix of signals. The directions of arrival of the d signals are $\theta_1, \theta_2, \dots, \theta_d$ respectively, so $\mathbf{A} = [\mathbf{a}_1 \ \mathbf{a}_2 \ \dots \ \mathbf{a}_d]$ is an $m \times d$ dimensional matrix. $\mathbf{S} = [\mathbf{s}_1 \ \mathbf{s}_2 \ \dots \ \mathbf{s}_d]^T$ is a $d \times L$ dimensional source signal matrix, where $\mathbf{s}_j = [s_{j,1} \ s_{j,2} \ \dots \ s_{j,L}]$ is the j -th source signal vector, $j = 1, 2, \dots, d$. \mathbf{N} is an $m \times L$ dimensional additive white Gaussian noise matrix.

3.2. Single-signal part in the overlapped signal

If the arrival time between the received ADS-B signals is less than the unit signal length, the time domain waveforms of these signals will overlap. These signals are called ADS-B overlapped signal. To reduce the probability of signals overlapping, the RTCA DO-260B protocol specifies that the time interval for different aircraft transmitting ADS-B signals is randomly selected within $0.4\text{--}0.6$ s (RTCA DO-260B, 2009). Hence, the probability of complete signal overlap is very small. There is a high probability of a certain TDOA between the overlapping signals. Therefore, the first and last signals to arrive in the overlapped signal are very special, since only these two signals may have non-overlapping parts, namely, the single-signal parts. Figure 1 illustrates the single-signal part in three overlapping signals. The curves from top to bottom in Figure 1 are the time-domain waveforms before and after the \mathbf{s}_1 , \mathbf{s}_2 , and \mathbf{s}_3 overlapping. The arrival times of the three signals are t_1 , t_2 , and t_3 , and their end times are t_4 , t_5 , and t_6 , respectively. Furthermore, the time-domain waveform of the overlapped signal is formed by the three signals' waveforms in order of their arrival.

Figure 1 shows that the samples of overlapped signal in the $t_1 \sim t_2$ period only contain \mathbf{s}_1 . \mathbf{s}_2 is completely overlapped because its start and end moments are within the duration of \mathbf{s}_1 and \mathbf{s}_3 . And the samples of the $t_5 \sim t_6$ period only contain \mathbf{s}_3 . Using the single-signal parts of the first (\mathbf{s}_1) and last signal (\mathbf{s}_3), we can separate the overlapped signal fast and efficiently.

The method for identifying the single-signal parts of the first and last signals in the overlapped signal is shown in Figure 2. We take samples of $1 \mu\text{s}$ as a segment from the beginning of overlapped signal and perform eigenvalue decomposition on each segment one by one. The noise power of the non-signal part is estimated as a threshold, and the number of eigenvalues bigger than the threshold is used as the estimation of the number of signal sources in different segments. When the number of signal sources

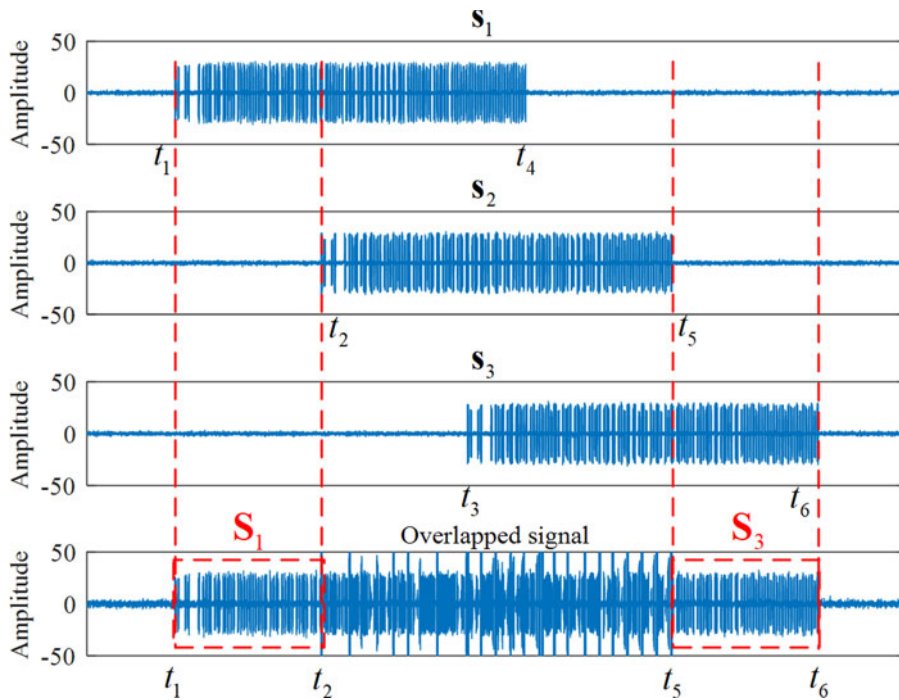


Figure 1. Schematic diagram of the single-signal part in the overlapped signal.

is bigger than one, we stop the eigenvalue decomposition and mark the sample. The samples with only one signal source are collected as the single-signal part of the first signal, denoted as \mathbf{X}_1 . The same operation is used to extract the single-signal part of the last signal. The $1 \mu\text{s}$ samples undergo eigenvalue decomposition one by one from the end of the overlapped signal. The samples with only one signal source are identified as the single-signal part of the last signal, denoted as \mathbf{X}_d .

3.3. Separate the first and last signals in the overlapped signal

After identifying the single-signal parts, we use them to estimate the steering vectors of the first and last signals in the overlapped signal. A constraint matrix is formed by the estimated steering vectors. We use the matrix to separate the first and last signals based on the LCMV algorithm (Xu et al., 2015). The LCMV algorithm finds the optimal weight matrix to minimise the output power of the beamformer under linearly constrained conditions. In the ADS-B signal separation problem, it is to find the optimal weight matrix that maximises the desired signal power while the output power of other signals is zero. Conventional beamforming methods such as Capon and minimum variance distortionless response algorithms can only form beams in one desired direction at a time. The LCMV algorithm can simultaneously form beams in multiple desired directions and form a zero limit in the interference direction. Hence, the paper applies the LCMV algorithm to the space-based ADS-B signal separation problem, which can separate the first and last signals at the same time.

The constrained equation of the LCMV algorithm can be expressed as

$$\begin{cases} \min_{\mathbf{W}} \mathbf{W}^H \mathbf{R} \mathbf{W} \\ \text{s.t. } \mathbf{C}^H \mathbf{W} = \mathbf{F} \end{cases} \quad (2)$$

where \mathbf{W} is the weighting matrix, \mathbf{R} is the covariance matrix of the received signal, \mathbf{C} is the constrained matrix consisting of spatial steering vectors corresponding to the constrained directions, and \mathbf{F} is a

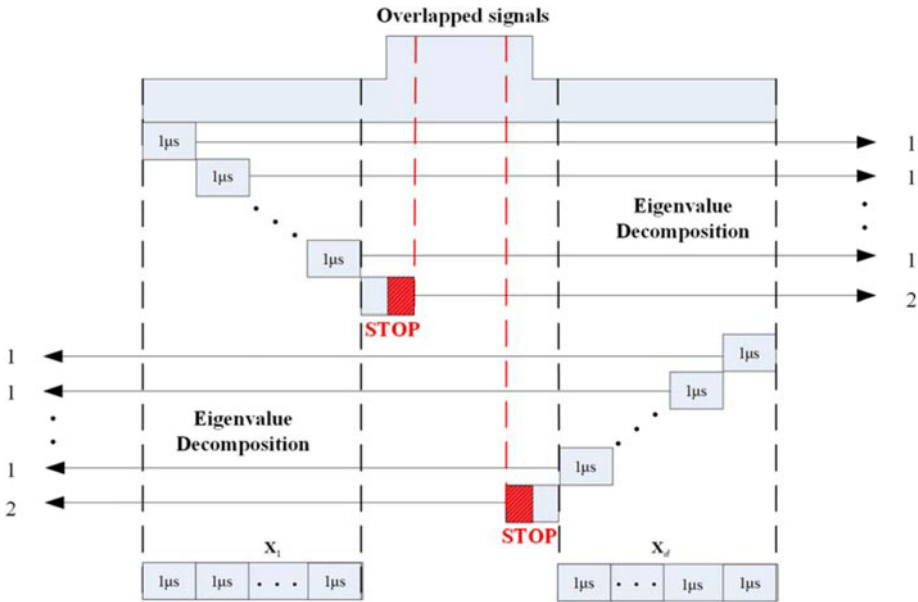


Figure 2. The process of identifying the single-signal part in the overlapped signal.

response matrix. After the single-signal parts in the overlapped signal are determined, \mathbf{X}_1 and \mathbf{X}_d are used to estimate the steering vectors of the first and last signal respectively. The constraint matrix \mathbf{C} is then formed by the estimated steering vectors $\hat{\mathbf{a}}_1$ and $\hat{\mathbf{a}}_d$ and can be expressed as

$$\mathbf{C} = [\hat{\mathbf{a}}_1, \hat{\mathbf{a}}_d] \tag{3}$$

To separate the first and last signals simultaneously, the response matrix should be set as $\mathbf{F} = \begin{bmatrix} 1 & 0 \\ 0 & 1 \end{bmatrix}$. Then Equation (2) can be transformed into the following optimisation problem:

$$\begin{cases} \min \sum_{i=1}^2 |\mathbf{w}_i^H \hat{\mathbf{a}}_i|^2 \\ s.t. \mathbf{W}^H \hat{\mathbf{a}}_1 = [1 \ 0]^T \\ s.t. \mathbf{W}^H \hat{\mathbf{a}}_d = [0 \ 1]^T \end{cases} \tag{4}$$

Based on the Lagrange multiplier method, the optimal weight matrix of Equation (4) can be solved as

$$\mathbf{W}_{opt} = \frac{\mathbf{R}^{-1} \mathbf{C}}{\mathbf{C}^H \mathbf{R}^{-1} \mathbf{C}} \cdot \mathbf{F} \tag{5}$$

Finally, after obtaining the separation matrix \mathbf{W}_{opt} by Equation (5), its transposed matrix is multiplied by \mathbf{X} to obtain the separated signals.

$$\mathbf{Y} = \mathbf{W}_{opt}^H \mathbf{X} = \begin{bmatrix} \hat{\mathbf{s}}_1 \\ \hat{\mathbf{s}}_d \end{bmatrix} \tag{6}$$

In Equation (6), each row of the matrix \mathbf{Y} corresponds to one separated signal, the first or last signal, in no particular order. If the number of signal sources in \mathbf{X} is greater than two, we should continue separating other signals.

Algorithm 1. OPLCMV algorithm for space-based ADS-B signal separation.

It is known that the total number of snapshots in the received signal \mathbf{X} is L . Suppose the number of signal sources in \mathbf{X} is d .

- 1: Preprocess the received signal matrix \mathbf{X} . Estimate d , if $d = 1$, the algorithm ends; if $d > 1$, \mathbf{X} needs to be separated, and the following operations should be performed. \mathbf{X} is projected onto the eigenvectors corresponding to the d largest eigenvalues, and the dimension of \mathbf{X} is reduced to d rows;
- 2: Estimate the single-signal parts \mathbf{X}_1 and \mathbf{X}_d of the first and last signals in \mathbf{X} ;
- 3: Use \mathbf{X}_1 and \mathbf{X}_d to estimate $\hat{\mathbf{a}}_1$ and $\hat{\mathbf{a}}_d$, the steering vectors of the first and last signals, and form a constraint matrix $\mathbf{C} = [\hat{\mathbf{a}}_1, \hat{\mathbf{a}}_d]$;
- 4: Calculate the separation matrix of the first and last signals based on the LCMV algorithm, $\mathbf{W} = \mathbf{R}^{-1}\mathbf{C}[\mathbf{C}^H\mathbf{R}^{-1}\mathbf{C}]^{-1}\mathbf{F}$, where $\mathbf{F} = \begin{bmatrix} 1 & 0 \\ 0 & 1 \end{bmatrix}$, \mathbf{R} is the sample covariance matrix of \mathbf{X} after preprocessing;
- 5: Let $\mathbf{Y} = \mathbf{W}^H\mathbf{X}$ separate the first and last signals, \mathbf{Y} is a $2 \times L$ dimensional matrix, each row of \mathbf{Y} corresponds to one separated signal, and the separation is in no order;
- 6: Project \mathbf{X} to the orthogonal space (\mathbf{P}^\perp) of the first and last signals, $\mathbf{P}^\perp = \mathbf{I} - \mathbf{C}(\mathbf{C}^H\mathbf{C})^{-1}\mathbf{C}^H$, and extract the remaining overlapped signal, $\mathbf{X}_r = \mathbf{P}^\perp \cdot \mathbf{X}$. If \mathbf{X}_r contains more than one signal, repeat steps 2~6 until all the signals are separated; if \mathbf{X}_r contains only one signal, output directly and the algorithm ends.

3.4. Extract the remaining overlapped signal

If the number of signal sources in \mathbf{X} is greater than two, the remaining overlapped signal needs to be extracted. The orthogonal projection matrix \mathbf{P}^\perp of the first and last signals is constructed and can be expressed as

$$\mathbf{P}^\perp = \mathbf{I} - \mathbf{C}(\mathbf{C}^H\mathbf{C})^{-1}\mathbf{C}^H \quad (7)$$

\mathbf{C} is the constraint matrix consisting of spatial steering vectors corresponding to the separated first and last signals, as shown in Equation (3).

\mathbf{X} is projected onto the orthogonal space of the first and last signals to obtain the remaining overlapped signal \mathbf{X}_r , as shown in Equation (8).

$$\mathbf{X}_r = \mathbf{P}^\perp \cdot \mathbf{X} \quad (8)$$

Finally, we need to determine the number of signal sources in \mathbf{X}_r . If \mathbf{X}_r contains only one signal, it is the last separated signal; if \mathbf{X}_r contains two or more signals, the new single-signal parts of the remaining overlapped signal should be determined and Equations (2)–(8) should be reused until all signals in \mathbf{X}_r are separated. The steps of the OPLCMV algorithm are shown in Algorithm 1.

4. Results and discussion

The simulation experiments are used to verify the performance of the OPLCMV algorithm in this paper. A uniform linear array with 12 elements is used as the receiving antenna. The input SNRs of all signals are 13 dB. The TDOAs between all signals are 10 μ s. But the number of overlapped signal sources is changed from two to ten, with a DDOA range between overlapped signals of -60° to 60° , and a carrier frequency difference range of -1 to 1 MHz. We validated the OPLCMV algorithm by investigating the number of overlapped signal sources, the DDOAs and frequency shifts between overlapping signals, the number of elements in the array antenna, and the calculation amount. Meanwhile, the OPLCMV algorithm is compared with the EPA and FastICA by using the decoding accuracy as an evaluation. The

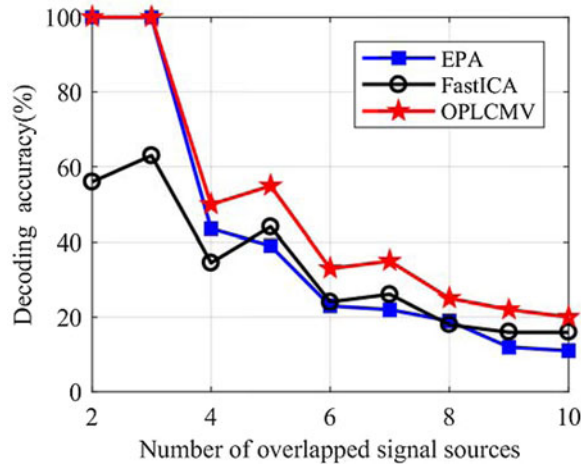


Figure 3. Decoding accuracy for different overlapped signal sources.

decoding accuracy is the percentage of the number of correctly decoded signals in the total number of received signals in 100 Monte Carlo experiments, which ranges from 0 % to 100 %. In the experiments, the number of overlapped signal sources and the TDOA between signals are assumed to be known. In practice, empirical mode decomposition (EMD) (Lu and Chen, 2019), singular value decomposition (Petrochilos et al., 2009) and eigenvalue decomposition can be used to estimate the number of overlapped signal sources.

4.1. Evaluation of ADS-B overlapped signal sources

The overlapped signal is simulated with a 3° DDOA step, the input SNR is 13 dB, the TDOA between all signals is $10 \mu\text{s}$, and the frequency shift between signals is 200 kHz. These parameters remain the same in this experiment, only the number of overlapped signal sources varies from two to ten. The OPLCMV algorithm, EPA and FastICA are used to separate from two to ten overlapping signals, respectively. The decoding accuracy of the three algorithms is shown in Figure 3.

From Figure 3, both the EPA and OPLCMV algorithm can separate the overlapped signals well for fewer signal sources, such as two or three overlapping signals, and the decoding accuracy of the FastICA algorithm is up to 63 %. As the number of overlapping signal sources increases, the decoding accuracy of all three algorithms decreases. However, the OPLCMV algorithm outperforms EPA and FastICA. The average decoding accuracy of the OPLCMV algorithm is $7 \cdot 83\%$ and $15 \cdot 83\%$ higher than that of the EPA and FastICA, respectively. Since the EPA separates the signals one by one from the beginning of the overlapped signal, it projects the overlapped signal onto the orthogonal space of the separated one to extract the remaining overlapped signal and repeats the process to separate other signals. When the number of overlapped signal sources increases and the DDOAs between signals are small, the continuous orthogonal projection to extract the remaining overlapped signal will inevitably cause losses to the components of the remaining signals. It will result in the misestimation of the steering vectors, and the remaining overlapped signals cannot be separated accurately. The FastICA algorithm uses the non-Gaussian property of the ADS-B signal to separate the overlapped signal by calculating the weighting matrix that maximises the negentropy of the overlapped signal. However, an initial value must be assigned to the weighting matrix, and this value determines the degree of convergence of the algorithm. When the number of overlapped signal sources is large, it is difficult to obtain an accurate weighting matrix, and the accuracy of the algorithm is reduced. The OPLCMV algorithm separates the first and last signals from the overlapped signal each time. Assume that the DDOAs between overlapping signals are all $\Delta\theta$ and there are d independent signals overlapping. The DDOA between the signals separated

by the EPA is $\Delta\theta$ each time, but the DDOA of the OPLCMV algorithm's first separation is $(d - 1)\Delta\theta$. So, the decoding accuracy of the OPLCMV algorithm is gradually higher than the EPA and FastICA algorithm when the number of overlapped signal sources increases. This means that the OPLCMV algorithm can correctly separate and decode a greater number of ADS-B overlapping signal sources than existing methods under the same conditions. Therefore, the OPLCMV algorithm can provide more accurate aircraft information for the ATC surveillance system and enhance aviation flight safety.

Meanwhile, it can be noticed from Figure 3 that the decoding accuracy of the three algorithms is the lowest for 10 overlapping signals. And in this case, the EPA and the FastICA algorithm can only separate 1 · 1 and 1 · 6 signals, while the OPLCMV algorithm can correctly separate two signals. The number of separated signals refers to the number of overlapping signal sources multiplied by the decoding accuracy of the three algorithms after 100 Monte Carlo experiments. The OPLCMV algorithm uses the single-signal parts and beamforming method to separate overlapped signals. Due to the presence of single-signal parts, the first and last signals can always be separated correctly. As a result, even with 10 overlapping signals in this experiment, the OPLCMV algorithm can still accurately separate the first and last signals. However, the remaining overlapping signals are separated by the beamforming method, and the decoding accuracy of the method depends on the relationship between the DDOAs of the remaining overlapping signals and the beamwidth of the receiving array antenna. If the DDOAs are larger than the beamwidth, all the remaining overlapping signals can be separated correctly. Otherwise, only a part of the signals can be separated. Therefore, the decoding accuracy of the OPLCMV algorithm decreases as the number of overlapped signal sources increases in this experiment. If we want to improve the decoding accuracy of the OPLCMV algorithm with 10 overlapping signals in this case, a greater number of receiving array antenna elements is required. For example, when the number of array antenna elements was increased from 12 to 20 and the beamwidth was reduced from $8 \cdot 5^\circ$ to $5 \cdot 1^\circ$, the OPLCMV algorithm was able to correctly separate 5 · 6 signals for 10 overlapping signals, while the EPA and FastICA algorithm only separate 3 · 7 and 4 · 7 signals, respectively.

4.2. Evaluation of DDOAs between overlapping signals

This section evaluates the OPLCMV algorithm by analysing the DDOAs between overlapping signals. Based on the performance of overlapped signal sources, we use 10 overlapping signals to evaluate the impact of DDOAs on signal separation. All signals have an input SNR of 13 dB, a TDOA of 10 μ s, and a frequency shift of 200 kHz. In this experiment, the DDOA between overlapping signals is the same and it varies from 0° to 10° . After 100 Monte Carlo experiments, the decoding accuracy of the OPLCMV algorithm, EPA and FastICA algorithm with different DDOAs are compared, as shown in Figure 4.

As shown in Figure 4, the decoding accuracy of the OPLCMV algorithm, EPA and FastICA algorithm all increase as the DDOA increases. In addition, the average decoding accuracy of the OPLCMV algorithm is 6 · 84% and 16 · 09% higher than that of the EPA and FastICA algorithm, respectively. When the DDOA is small, such as below 6° , the decoding accuracy of the OPLCMV algorithm is significantly higher than that of the EPA and FastICA algorithm. When the DDOA is greater than 8° , both the EPA and OPLCMV algorithm can separate the signals well. This also confirms the conclusion in Section 4.1 that the OPLCMV algorithm can effectively separate all the signals when the DDOAs between remaining overlapping signals are larger than the beamwidth of the receiving array antenna. However, the decoding accuracy of the FastICA algorithm is still less than 80%. According to Figure 4, the OPLCMV algorithm outperforms the EPA and FastICA algorithm and is more suitable for small DDOA.

4.3. Evaluation of frequency shifts between overlapping signals

To avoid ADS-B 1090ES signal overlapping, the ICAO stipulates that the carrier frequencies of different aircraft are randomly selected in the range of 1,089–1,091 MHz, so the maximum carrier frequency shift between ADS-B signals is 2 MHz. In order to investigate the impact of frequency shift between

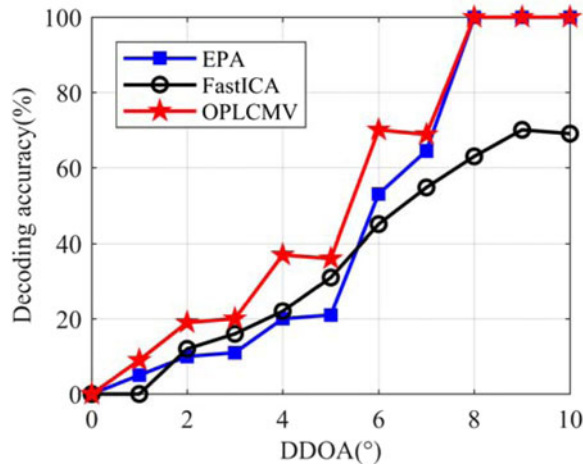


Figure 4. Decoding accuracy of overlapped signal with different DDOAs.

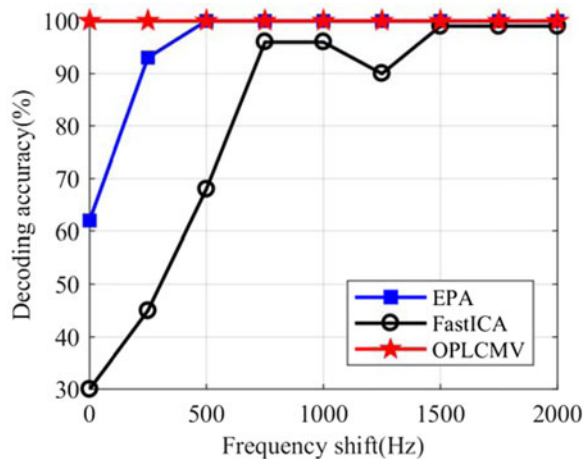


Figure 5. Decoding accuracy of overlapped signal with different frequency shifts.

overlapped signals on the OPLCMV algorithm, we fixed the number of overlapped signal sources at two, set the input SNR to 13 dB for both signals, and used a DDOA of 10° and a TDOA of $10\ \mu\text{s}$. The frequency shift between the two overlapping signals is changed from 0 to 2,000 Hz. Comparisons between the OPLCMV algorithm, EPA and FastICA algorithm with different frequency shifts are shown in Figure 5.

From Figure 5 it can be seen that the OPLCMV algorithm performs well in separating overlapped signals with different frequency shifts, and its average decoding accuracy is 5% and 19.78% higher than that of EPA and FastICA, respectively. In particular, the decoding accuracy of the OPLCMV algorithm is much higher than that of the EPA and the FastICA algorithm at small frequency shifts such as 0 to 500 Hz. Therefore, the OPLCMV algorithm is more appropriate for space-based ADS-B overlapped signals since it can effectively separate a greater number of signals when the frequency shift between overlapping signals is small.

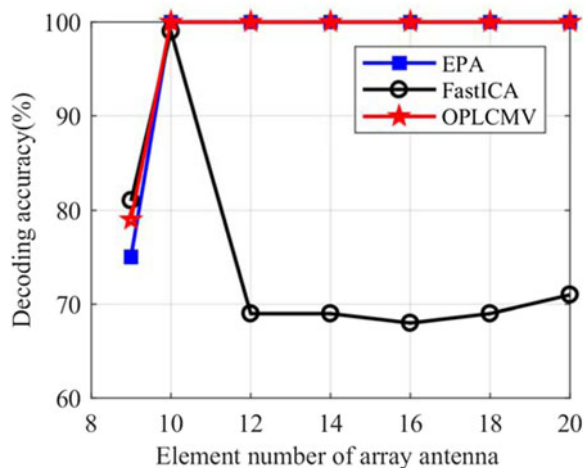


Figure 6. Decoding accuracy of the algorithms with different array antenna elements.

4.4. Evaluation of the number of elements of array antenna

In previous experiments, the receiving antenna was a uniform linear array with 12 elements. To evaluate the influence of the number of elements of the array antenna, we list the decoding accuracy of the OPLCMV algorithm, EPA and FastICA algorithm with different receiving array antenna elements. Ten overlapping signals are used, and the input SNR of all signals is 13 dB. The DDOA is 10° , the TDOA is $10 \mu\text{s}$ and the frequency shift is 200 kHz. Figure 6 shows the decoding accuracy of the three algorithms after 100 Monte Carlo experiments as the number of elements in the array antenna increases from nine to twenty.

Figure 6 shows that when the number of array antenna elements varies from nine to twenty, the average decoding accuracy of the OPLCMV algorithm, the EPA and the FastICA algorithm is 97%, 96.43% and 75.14%, respectively. However, the decoding accuracy of all three algorithms drops drastically when the number of array antenna elements is smaller than the number of overlapped signal sources, and it has the greatest impact on the EPA. When the number of array antenna elements is equal to or greater than the number of overlapped signal sources, it has little effect on the decoding accuracy of the EPA and OPLCMV algorithm, both algorithms can achieve better decoding accuracy. Besides, the FastICA algorithm achieves the highest accuracy when the number of elements is equal to the number of overlapped signal sources.

Meanwhile, it also can be concluded from Section 4.1, Section 4.2 and Section 4.4 that when the DDOAs between overlapped signal are larger than the beamwidth of the receiving antenna, the number of receiving array antenna elements has little influence on the decoding accuracy of OPLCMV algorithm. However, the decoding accuracy and the number of separated signals of the OPLCMV algorithm can be improved by increasing the number of receiving antenna elements when the DDOA is smaller than the beamwidth of the receiving antenna.

4.5. Calculation amount of the OPLCMV algorithm

The effectiveness of the OPLCMV algorithm has been verified from the number of overlapped signal sources, DDOA and frequency shift between overlapping signals, and the number of array antenna elements respectively in the above four experiments. This section compares the OPLCMV algorithm with the EPA from the perspective of the calculation amount. Both the OPLCMV algorithm and EPA utilise the features of the single-signal part in the ADS-B overlapped signal. However, the EPA separates the signals one by one from the beginning of the overlapped signal, while the OPLCMV algorithm

Table 1. Comparison of calculation amount.

	EPA	OPLCMV
Multiplication	$[d^2(t_2 - t_1) + (d - 1)^2(t_3 - t_2) + \dots + 2^2(t_d - t_{d-1})] \cdot f_s$ $+ \sum_{n=2}^d \left[\frac{1}{2}n^2(7L + 5) + \frac{1}{2}n(L + 2n! + 7) + L \right]$	<p>d is odd,</p> $\frac{1}{2}d^3(L + 8)$ $+ \frac{1}{2}d^2(5L - 2L_0 + 4d! + 18)$ $- d(L + d! - 6) - 16$ <p>d is even,</p> $\frac{1}{2}d^3(L + 8)$ $+ d^2(2L + L_d - L_0 + 2d! + 11)$ $+ 8d - 16, \text{ where}$ $L_d = \left(\frac{t_{d+2} - t_d}{2} \right) \cdot f_s$
Addition	$[d^2(t_2 - t_1) + (d - 1)^2(t_3 - t_2) + \dots + 2^2(t_d - t_{d-1})] \cdot f_s$ $+ \sum_{n=2}^d \left[n! + \frac{1}{2}n^2(6L - 3) - \frac{1}{2}n(2L - 3) - 2 \right]$	<p>d is odd,</p> $\frac{1}{2}d^3(L + 6) + d^2(2L - L_0 + 1)$ $- \frac{1}{2}d(3L - 4d! + 20) + L + 3$ <p>d is even,</p> $\frac{1}{2}d^3(L + 6) + \frac{1}{2}d^2(3L + 2L_d - 2L_0 + 4)$ $+ d(d! - 10) + (d + 1)! + 2$

separates signals from the beginning and the end of the overlapped signal at the same time, two signals are separated at each time.

Assuming that d is the number of overlapped signal sources received, the arrival times of these d signals are denoted by t_1, t_2, \dots, t_d , respectively. The sampling frequency of the receiver is represented by f_s , which is a fixed constant. $L_0 = 120 \mu s \times f_s$ is the number of unit signal snapshots. So, the total number of the received signal snapshots is $L = (t_d - t_1 + 120 \mu s) \cdot f_s$. Therefore, the calculation amounts of the EPA and OPLCMV algorithms under the same condition are compared in Table 1. It should be pointed out that the calculation amount of the OPLCMV algorithm is decided by the parity of the number of the overlapped signal sources.

Suppose the TDOA between the overlapping signals is $10 \mu s$, and the receiver sampling frequency (f_s) is 40 MHz. Using the calculation equations provided in Table 1 for the EPA and OPLCMV algorithm, we can determine the number of complex multiplications and additions, required to separate two to eight overlapping signals under these conditions. The number of complex multiplications and additions are shown in Figure 7.

Figure 7 illustrates that the number of complex multiplications and additions required by the OPLCMV algorithm is only 0.55 times that of the EPA when the number of overlapped signal sources

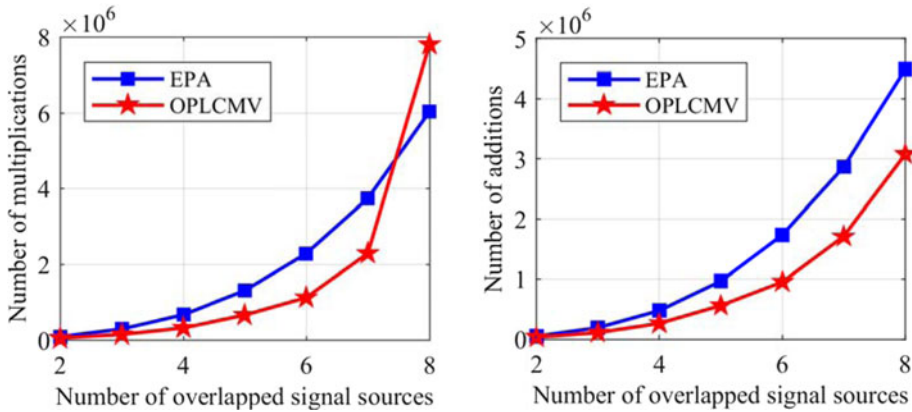


Figure 7. Comparison of the calculation amount between the EPA and the OPLCMV algorithm: (a) multiplication, (b) addition.

is less than seven. Since the OPLCMV algorithm can separate two signals in each iteration, and EPA can only separate one signal, the number of iterations of the OPLCMV algorithm is about half that of the EPA. However, the OPLCMV algorithm requires matrix inversion when calculating the separation matrix, and the dimension of the received signal matrix is unchanged in every iteration. With the dimension of the received signal matrix in EPA decreasing in every iteration, the calculation of the matrix inversion gradually reduces. Therefore, OPLCMV algorithm has lower computational cost than the EPA when dealing with a small number of overlapped signal sources, and its calculation amount gradually exceeds that of EPA as the number of overlapped signal sources increases. Nevertheless, the OPLCMV algorithm still achieves higher decoding accuracy than the EPA.

5. Conclusions

This paper proposes an OPLCMV algorithm for space-based ADS-B signal separation, which is suitable for separating multiple overlapping signals with small DDOAs or small frequency shifts. Based on the characteristics of the ADS-B overlapping signals, the OPLCMV algorithm uses the single-signal parts to separate two signals simultaneously until all signals are separated. The evaluation of the proposed method takes into account the number of overlapped signal sources, as well as the DDOA and frequency shift between overlapping signals, in addition to the number of receiving array antenna elements. Simulation experiments verify the effectiveness of the OPLCMV algorithm. It has higher decoding accuracy than the EPA and the FastICA algorithm for more multiple overlapping signals, small DDOAs and small frequency shifts. Moreover, the calculation amount of the OPLCMV algorithm is about half of the EPA when the number of overlapped signal sources is less than seven. Therefore, the proposed OPLCMV algorithm can separate space-based ADS-B overlapped signals with higher accuracy and speed.

The practical application of the algorithm will be considered in future work. Since the proposed algorithm is based on a multi-antenna array to separate the ADS-B overlapping signals, an array antenna and a multi-channel acquisition system are required to receive ADS-B signals in the field test. However, the algorithm is blind beamforming, it does not need to know the array manifold and is easy to use. The steps of the proposed algorithm separating the real overlapping signals are as follows. Firstly, an array antenna is utilised to receive the overlapped signals. Secondly, the signals are converted and sampled by a radio frequency front-end to obtain the digital baseband signals. Thirdly, the baseband signals are input into the proposed algorithm to separate the overlapped signals. Finally, a software receiver is used to decode the separated signals and retrieve ADS-B information. To reduce the overlap probability of ADS-B signals, many companies employ multi-antenna designs on space-based ADS-B

receivers (Blomenhofer et al., 2012; Bettray et al., 2013; Yu et al., 2020; Zhao et al., 2022). Therefore, the proposed algorithm can be directly applied to space-based ADS-B receivers.

Funding statement. This work is supported by the Civil Aviation Joint Research Fund of the National Natural Science Foundation of China under grant number U2133204, and the Scientific Research Programme of Tianjin Municipal Education Commission under grant number 2021KJ042.

References

- Ali, B. S. (2016). System specifications for developing an automatic dependent surveillance-broadcast (ADS-B) monitoring system. *International Journal of Critical Infrastructure Protection*, **15**, 40–46.
- Ali, B. S., Schuster, W. and Ochieng, W. Y. (2017). Evaluation of the capability of automatic dependent surveillance broadcast to meet the requirements of future airborne surveillance applications. *Journal of Navigation*, **70**, 49–66.
- Baek, J., Hableel, E., Byon, Y. J., Wong, D. S., Jang, K. and Yeo, H. (2016). How to protect ADS-B: Confidentiality framework and efficient realization based on staged identity-based encryption. *IEEE Transactions on Intelligent Transportation Systems*, **18**(3), 690–700.
- Baker, K. (2019). Space-Based ADS-B: Performance, Architecture and Market. *Proceedings of the 2019 Integrated Communications, Navigation and Surveillance Conference*, Herndon, VA.
- Bettray, A., Litschke, O. and Baggen, L. (2013). Multi-Beam Antenna for Space-Based ADS-B. *Proceedings of the 2013 IEEE International Symposium on Phased Array Systems and Technology*, Waltham, MA.
- Blomenhofer, H., Pawlitzki, A., Rosenthal, P. and Escudero, L. (2012). Space-Based Automatic Dependent Surveillance Broadcast (ADS-B) Payload for In-Orbit Demonstration. *Proceedings of the 6th Advanced Satellite Multimedia Systems Conference and 12th Signal Processing for Space Communications Workshop*, Vigo, Spain.
- Carandente, M. and Rinaldi, C. (2014). Aireon Surveillance of the Globe via Satellite. *Proceedings of the 2014 Tyrrhenian International Workshop on Digital Communications - Enhanced Surveillance of Aircraft and Vehicles*, Rome, Italy.
- Chen, L., Yu, S., Chen, Q. and Zhao, Y. (2020). Data reception analysis of ADS-B on board the Tiantuo-3 satellite. *Journal of Physics: Conference Series*, **1438**(1), 012030.
- Galati, G., Petrochilos, N. and Piracci, E. G. (2015). Degarbling mode S replies received in single channel stations with a digital incremental improvement. *IET Radar, Sonar and Navigation*, **9**(6), 681–691.
- Garcia, M. A., Dolan, J. and Hoag, A. (2017). Aireon's Initial On-Orbit Performance Analysis of Space-Based ADS-B. *Proceedings of the 2017 Integrated Communications, Navigation and Surveillance Systems Conference*, Herndon, VA.
- Garcia, M. A., Dolan, J., Haber, B., Hoag, A. and Diekelman, D. (2018). A Compilation of Measured ADS-B Performance Characteristics from Aireon's On-Orbit Test Program. *Proceedings of the 2018 Enhanced Solutions for Aircraft and Vehicle Surveillance Applications Conference*, Berlin, Germany.
- Knudsen, B. G., Jensen, M., Birklykke, A., Koch, P., Christiansen, J., Laursen, K., Almide, L. and Le Moullec, Y. (2014). ADS-B in Space: Decoder Implementation and First Results from the GATOSS Mission. *Proceedings of the 14th Biennial Baltic Electronic Conference*, Tallinn, Estonia.
- Liu, K., Zhang, T. and Ding, Y. (2016). Blind Signal Separation Algorithm for Space-Based ADS-B. *Proceedings of the 2016 International Conference on Mechatronics Engineering and Information Technology*, Xi'an, China.
- Liu, H. T., Wang, S. L., Qin, D. B. and Li, D. X. (2018). Performance analysis of surveillance capacity of satellite-based ADS-B receiver. *Acta Aeronautica et Astronautica Sinica*, **39**(5), 321866. (In Chinese).
- Lu, D. and Chen, T. (2019). Single-antenna overlapped ADS-B signal self-detection and separation algorithm based on EMD. *Journal of Signal Processing*, **35**(10), 1680–1689. (In Chinese).
- Lu, F., Chen, Z. and Chen, H. (2021). Lateral collision risk assessment of parallel routes in ocean area based on space-based ADS-B. *Transportation Research Part C: Emerging Technologies*, **124**, 102970.
- Mangali, N. K. and Bagmare, V. S. (2017). Development of a Power over Ethernet (PoE) Enabled ADS-B Receiver System. *2017 International Conference on Wireless Communications, Signal Processing and Networking*, Chennai, India.
- Nies, G., Stenger, M., Krčál, J., Hermanns, H., Bisgaard, M., Gerhardt, D., Haverkort, B., Jongerden, M., Larsen, K. G. and Wognsen, E. R. (2018). Mastering operational limitations of LEO satellites – the GOMX-3 approach. *Acta Astronautica*, **151**, 726–735.
- Petrochilos, N. and Van Der Veen, A. J. (2007). Algebraic algorithms to separate overlapping secondary surveillance radar replies. *IEEE Transactions on Signal Processing*, **55**(7), 3746–3759.
- Petrochilos, N., Galati, G. and Piracci, E. (2009). Separation of SSR signals by array processing in multilateration systems. *IEEE Transactions on Aerospace and Electronic Systems*, **45**(3), 965–982.
- RTCA DO-260B. (2009). Minimum Operational Performance Standards for 1090 MHz Extended Squitter Automatic Dependent Surveillance–Broadcast (ADS-B) and Traffic Information Services–Broadcast (TIS-B). Radio Technical Commission for Aeronautics (RTCA), Washington, DC.
- Vincent, R. and Freitag, K. (2019). The Canx-7 ADS-B mission: signal propagation assessment. *Positioning*, **10**(1), 1–15.
- Wang, W., Wu, R. and Liang, J. (2019). ADS-B signal separation based on blind adaptive beamforming. *IEEE Transactions on Vehicular Technology*, **68**(7), 6547–6556.

- Werner, K., Bredemeyer, J. and Delovski, T.** (2014). ADS-B Over Satellite: Global Air Traffic Surveillance from Space. *Proceedings of the 2014 Tyrrhenian International Workshop on Digital Communications - Enhanced Surveillance of Aircraft and Vehicles*, Rome, Italy.
- Wu, S., Chen, W. and Chao, C.** (2016). The STU-2 CubeSat Mission and in-Orbit Test Results. *Proceedings of the 30th Annual AIAA/USU Conference on Small Satellites*, Logan, UT.
- Xu, J., Liao, G., Zhu, S. and Huang, L.** (2015). Response vector constrained robust LCMV beamforming based on semidefinite programming. *IEEE Transactions on Signal Processing*, **63**(21), 5720–5732.
- Yu, S., Chen, L., Li, S. and Li, L.** (2018). Separation of Space-Based ADS-B Signals with Single Channel for Small Satellite. *Proceedings of the 2018 IEEE 3rd International Conference on Signal and Image Processing*, Shenzhen, China.
- Yu, S., Chen, L., Li, S. and Zhang, X.** (2019). Adaptive multi-beamforming for space-based ADS-B. *Journal of Navigation*, **72**(2), 359–374.
- Yu, S., Chen, L., Fan, C., Ding, G., Zhao, Y. and Chen, X.** (2020). Integrated antenna and receiver system with self-calibrating digital beamforming for space-based ADS-B. *Acta Astronautica*, **170**, 480–486.
- Zhang, Z.** (2018). Optimization performance analysis of 1090ES ADS-B signal separation algorithm based on PCA and ICA. *International Journal of Performability Engineering*, **14**(4), 741–750.
- Zhang, Y., Li, W. and Dou, Z.** (2019). Performance Analysis of Overlapping Space-Based ADS-B Signal Separation Based on FastICA. *Proceedings of the 2019 IEEE Globecom Workshops*, Waikoloa, HI.
- Zhao, Y., Wang, N., Chen, Q., Yu, S. and Chen, X.** (2022). Satellite coverage traffic volume prediction using a new surrogate model. *Acta Astronautica*, **193**, 357–369.
- Zhou, K., Sun, X., Huang, H., Wang, X. and Ren, G.** (2017). Satellite single-axis attitude determination based on automatic dependent surveillance-broadcast signals. *Acta Astronautica*, **139**, 130–140.